Article

Charge Recombination in Excited Donor-Acceptor Complexes with Two Absorption Bands

IONKIN, V. N., IVANOV, A. I., VAUTHEY, Eric

Abstract

The dynamics of charge recombination in a photoexcited donor-acceptor complex comprising 1,2,4-trimethoxybenzene (electron donor) and tetracyanoethylene (electron acceptor) in several polar solvents (acetonitrile, valeronitrile, and octanonitrile) was studied in terms of the stochastic approach. The Gibbs energy of charge recombination and the reorganization energies of the medium and quantum and vibrational degrees of freedom were found by fitting the stationary absorption spectrum. The electronic couplings were determined by analyzing the time dependences of the population of the ionic state in acetonitrile. A comparison of the numerical simulation results with the experimental data showed that the nonstationary model under consideration quantitatively described the dynamics of charge recombination and its dependence on the carrier frequency of excitation pulses and the relaxation properties of solvents.

Reference

IONKIN, V. N., IVANOV, A. I., VAUTHEY, Eric. Charge Recombination in Excited Donor-Acceptor Complexes with Two Absorption Bands. *Russian journal of physical chemistry*, 2009, vol. 83, no. 4, p. 683-688

DOI : 10.1134/S0036024409040281

ISSN 0036-0244, Russian Journal of Physical Chemistry A, 2009, Vol. 83, No. 4, pp. 683–688. © Pleiades Publishing, Ltd., 2009.
Original Russian Text © V.N. Ionkin, A.I. Ivanov, E. Vauthey, 2009, published in Zhurnal Fizicheskoi Khimii, 2009, Vol. 83, No. 4, pp. 791–797.

PHOTOCHEMISTRY AND MAGNETOCHEMISTRY

Charge Recombination in Excited Donor-Acceptor Complexes with Two Absorption Bands

V. N. Ionkin[a], A. I. Ivanov[a], and E. Vauthey[b]

[a] *Volgograd State University, Vtoraya Prodol'naya ul. 30, Volgograd, 400062 Russia*
[b] *Geneva University, Geneva, Switzerland*
e-mail: physic@vlink.ru; eric.vauthey@chiphy.unige.ch

Received April 10, 2008

Abstract—The dynamics of charge recombination in a photoexcited donor-acceptor complex comprising 1,2,4-trimethoxybenzene (electron donor) and tetracyanoethylene (electron acceptor) in several polar solvents (acetonitrile, valeronitrile, and octanonitrile) was studied in terms of the stochastic approach. The Gibbs energy of charge recombination and the reorganization energies of the medium and quantum and vibrational degrees of freedom were found by fitting the stationary absorption spectrum. The electronic couplings were determined by analyzing the time dependences of the population of the ionic state in acetonitrile. A comparison of the numerical simulation results with the experimental data showed that the nonstationary model under consideration quantitatively described the dynamics of charge recombination and its dependence on the carrier frequency of excitation pulses and the relaxation properties of solvents.

DOI: 10.1134/S0036024409040281

INTRODUCTION

The photoexcitation of charge-transfer bands in donor–acceptor complexes results in the formation of contact ion-radical pairs, whose destiny is determined by the competition of two processes, recombination to the ground state and the formation of free ions. These processes, like many other chemical reactions, are based on electron transfer [1].

Studies of the kinetics of recombination of donor-acceptor complexes showed that its rate k_{CR} monotonically increased as the energy gap separating the excited from ground state decreased [2–8]. It could be described by the equation $\ln k_{CR} = a + b\Delta G_{CR}$ [2], where ΔG_{CR} is the Gibbs energy of charge recombination and a and b are some constants. For the majority of complexes, the slope is ~1.34 decades per 1 eV. This behavior is qualitatively different from the bell-shaped dependence predicted by Marcus [9] and shows that the mechanism of recombination of excited donor-acceptor complexes differs from the Marcus mechanism, at least in the normal region, where the Gibbs energy of recombination is smaller than the energy of medium reorganization.

The trends observed in the recombination of excited donor-acceptor complexes were explained on the assumption that an important role was played by the nonequilibrium state of the medium formed under the action of short exciting pulses [10]. The original model [10] only included the reorganization of classical medium modes and predicted recombination to be strongly nonexponential, whereas an almost exponential kinetics was observed experimentally. It was shown in [11–13] that the inclusion of the reorganization of quantum high-frequency vibrational modes of complexes made the kinetics of recombination closer to exponential. It was in addition found that the nonadiabatic model (transitions between diabatic states induced by comparatively weak interactions between them) that took into account the nonequilibrium state of the medium and the reorganization of high-frequency modes (let us call it model A) gave a quantitative description not only of the kinetics of recombination but also of its dependence on the dynamic properties of solvents and the carrier frequency of exciting pulses [13].

There is also an alternative model (model B), which explains a monotonic increase in the rate of donor-acceptor complex recombination as the energy gap decreases on the assumption that the interaction between diabatic states is strong, and donor-acceptor complex recombination should be treated as the transition between the upper and lower adiabatic states induced by the nonadiabaticity operator [14–16]. Both models give a quite satisfactory explanation of the observed dependence of the rate k_{CR} on the energy gap width. It therefore remains to determine which of the two mechanisms operates in particular donor-acceptor complexes. Experimental observation of trends characteristic of only one model would answer this question. One of such trends is related to the two-stage character of recombination. At the first stage, recombination occurs in parallel with nuclear relaxation and, being nonequilibrium, is nonexponential. The second stage occurs after nuclear relaxation and is stationary. In

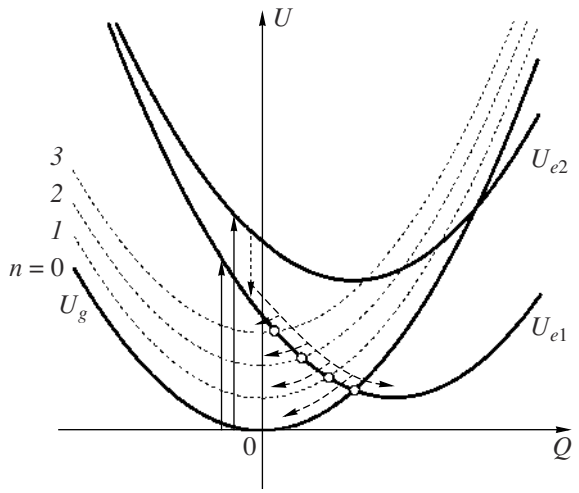

Fig. 1. Terms of donor-acceptor complex states participating in transitions with the excitation of the CT1 and CT2 bands (vertical arrows). The dotted arrow is the radiationless transition. Dotted lines are vibrational sublevels of the ground electronic state. Dashed arrows show the directions of system relaxation before and after nonthermal transitions.

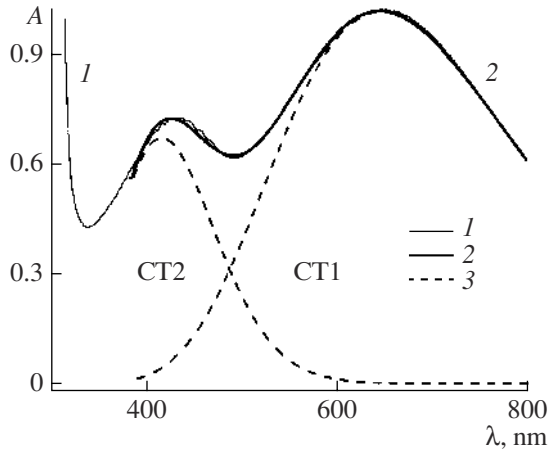

Fig. 2. (*1*) Stationary optical absorption spectrum of TMB/TCNE in ACN and (*2*) its approximation by the sum of two terms of type (12); (*3*) CT1 and CT2 bands.

model B, the rate at the second stage is always higher than at the first stage [15], whereas both variants are possible for model A. In particular, for reactions in the normal Marcus region, the rate of recombination at the thermal stage can be much lower than at the nonthermal stage because of the higher energy barrier that separates the ionic and neutral states. Although this prediction of model A almost never finds support in experimental data, this by itself is not a strong argument against this model, because the overwhelming majority of transitions can occur at the nonthermal stage; as a result, the thermal stage can be unobservable [11, 13].

The dynamics of charge recombination in the complex between 1,2,4-trimethoxybenzene (TMB) and tetracyanoethylene (TCNE) in several polar solvents was studied in [17]. This complex is characterized by two charge-transfer absorption bands (CT1 and CT2) with maxima at 655 and 434 nm, respectively. A study of the dynamics of recombination of the photoexcited complex in acetonitrile (ACN) revealed its two-stage character. The first stage was very fast, and the second, slow. In more viscous solvents, the reaction terminated at the fast stage and was independent of the exciting pulse wavelength. The decay of the charge transfer state in ACN after excitation at 620 nm was characterized by effective time of 30–80 fs, and the signal at times on the order of 0.5 ps faded away almost to zero. When TMB/TCNE was excited by a pulse at 480 nm, the two-stage character of decay dynamics was most pronounced. The first stage was characterized by the time as short as in the previous case, whereas the second stage was slow, and its characteristic time was substantially longer than 100 ps.

The purpose of this work was to study the recombination dynamics of excited TMB/TCNE complexes in several polar solvents and the influence of the pumping pulse wavelength on it theoretically in terms of model A.

A MODEL OF SUPERFAST CHARGE RECOMBINATION IN DONOR–ACCEPTOR COMPLEXES WITH TWO ABSORPTION BANDS

The complex under consideration consisting of TMB and TCNE belongs to a vast group of donor–acceptor complexes with two charge transfer absorption bands [17, 18]. These bands are supposed to correspond to two transitions into different donor–acceptor complex electronic states. The transitions corresponding to the CT1 and CT2 bands are characterized by different sets of electron transfer energy parameters and likely lead to complexes with different geometries [18].

A scheme of the electronic terms that participate in transitions when the CT1 and CT2 bands are excited is shown in Fig. 1. The excitation of the donor–acceptor complex by a pulse with the wavelength 620 nm causes population of only the U_{e1} term (see Fig. 2). Charge recombination should then closely resemble recombination in complexes with one absorption band well described by two-level models. A more complex situation arises when the donor–acceptor complex is excited by a 480 nm pulse. Such a pulse causes the formation of wave packets on terms of both excited states U_{e1} and U_{e2} because of the overlapping of the CT1 and CT2 bands in this spectral region. The difference of the evolution of the wave packet created at the U_{e1} term from the case considered above is only caused by the difference of the initial positions of the wave packets. The excited state at the U_{e2} term has more possible evolution paths. First, direct charge recombination (direct transition from the $|e2\rangle$ into ground state) is possible. It was, however, shown in [17] that such a transition would

occur much more slowly than the transition observed experimentally because of a large energy gap width. Secondly, there can be radiationless transition from $|e2\rangle$ to $|e1\rangle$. This transition is close to vertical if the time of the transition is much shorter than the solvent relaxation time. Excess energy is then transferred to intramolecular complex vibrations.

We assume that the wave packet created at the U_{e2} term experiences an instantaneous vertical transition to the U_{e1} term. This means that we ignore the difference in wave packet motion at the U_{e1} and U_{e2} terms at times of the radiationless transition between these states. This approximation reduces calculations of the dynamics of charge recombination in the three-level model under consideration to calculations in terms of the two-level model described in detail in [11, 13].

The diabatic Gibbs energy surfaces of the ground and two excited states can be written in the Q_i coordinates as

$$U_g^{(n)} = \frac{1}{2}\sum_{i=1}^{m} Q_i^2 + n\hbar\Omega, \quad (1)$$

$$U_{e1} = \frac{1}{2}\sum_{i=1}^{m} (Q_i - (2E_{ri}^{(1)})^{1/2})^2 - \Delta G_{CR}^{(1)}, \quad (2)$$

$$U_{e2} = \frac{1}{2}\sum_{i=1}^{m} (Q_i - (2E_{ri}^{(2)})^{1/2})^2 - \Delta G_{CR}^{(2)}. \quad (3)$$

Here, Ω is the frequency of the intramolecular vibrational mode and $E_{ri}^{(j)}$ is the reorganization energy of the ith solvent mode for the transition from the ground to jth excited state. This energy is related to its weight x_i in the relaxation function (4) as $x_i = E_{ri}^{(j)}/E_r^{(j)}$, $E_r^{(j)} = \sum_i E_{ri}^{(j)}$.

The introduction of multidimensional surfaces allows us to describe chemical transformations in media characterized by several relaxation times τ_i [19–21]. These times are usually associated with different relaxation modes, and the medium relaxation function $X(t)$ is written in the form

$$X(t) = \sum_{i=1}^{m} x_i e^{-t/\tau_i}, \quad \sum_{i=1}^{m} x_i = 1, \quad (4)$$

where m is the number of relaxation modes. It is known that a random process with an autocorrelation function of type (4) can be represented as a multidimensional random process with one-exponential autocorrelation functions $\exp(-t/\tau_i)$ in each dimension [22]. An independent reaction coordinate, Q_i, can be put in correspondence to each process. This makes it possible to describe the relaxation of a system by diffusion equations along each coordinate.

In the suggested approach, the evolution of the system is described by Liouville stochastic equations [23, 24] for the probability distribution function of finding a particle in the vicinity of the point $(Q_1, \ldots, Q_m)$ at time t at the excited state term $\rho_{e1}(Q_1, \ldots, Q_m, t)$ and at the nth sublevel of the ground state term $\rho_g^{(n)}(Q_1, \ldots, Q_m, t)$,

$$\frac{\partial \rho_{e1}}{\partial t} = \hat{L}_e \rho_{e1} - \sum_n k_{nj}(Q_1, \ldots, Q_m)(\rho_{e1} - \rho_g^{(n)}), \quad (5)$$

$$\frac{\partial \rho_g^{(n)}}{\partial t} = \hat{L}_g \rho_g^{(n)} - k_{nj}(Q_1, \ldots, Q_m)(\rho_g^{(n)} - \rho_{e1}) + \frac{1}{\tau_v^{(n+1)}}\rho_g^{(n+1)} - \frac{1}{\tau_v^{(n)}}\rho_g^{(n)}. \quad (6)$$

Here, $\hat{L}_g$ and $\hat{L}_{e1}$ are the Smoluchowski operators describing diffusion motion at the terms U_g, including its oscillatory repetitions, and U_{e1}, respectively,

$$\hat{L}_g = \sum_{i=1}^{m} \frac{1}{\tau_i}\left(1 + Q_i\frac{\partial}{\partial Q_i} + \langle Q_i^2\rangle \frac{\partial^2}{\partial Q_i^2}\right),$$
$$\hat{L}_{e1} = \sum_{i=1}^{m} \frac{1}{\tau_i}\left(1 + (Q_i - (2E_{ri}^{(1)})^{1/2})\frac{\partial}{\partial Q_i} + \langle Q_i^2\rangle \frac{\partial^2}{\partial Q_i^2}\right), \quad (7)$$

where $\langle Q_i^2\rangle = k_B T$ is the variance of the equilibrium distribution along the corresponding coordinate, k_B is the Boltzmann constant, and T is the temperature. It is also assumed that the mechanism of relaxation of high-frequency vibrations is one-quantum, and only transitions between neighboring vibrational sublevels $n \longrightarrow n-1$ occur at a rate of $1/\tau_v^{(n)}$. We also assume that

$$\tau_v^{(n)} = \tau_v^{(1)}/n, \quad (n = 1, 2, \ldots). \quad (8)$$

This dependence is substantiated in [12].

Electronic transitions between the excited state $|e1\rangle$ and the nth vibrational sublevel of the ground state $|g\rangle$ are described by the rates $k_{nj}(Q_1, \ldots, Q_m)$, which, according to [23, 24], have the form

$$k_{nj} = \frac{2\pi V_{nj}^2}{\hbar}\delta(U_{e1} - U_g^{(n)}) = \frac{2\pi V_{nj}^2}{\hbar}\delta(z - z_n^{\dagger}),$$
$$V_{nj}^2 = V_{elj}^2 F_{n1}, \quad F_{n1} = \frac{S_1^n e^{-S_1}}{n!}. \quad (9)$$

Here, $z = \sum (2E_{ri}^{(1)})^{1/2} Q_i$ is the collective energy coordinate of the reaction, $z_n^{\dagger} = E_r^{(1)} + \Delta G_{CR}^{(1)} - n\hbar\Omega$ denotes U_{e1}, $U_n^{(g)}$ term crossing points, F_{nj} is the Frank–Condon factor, $S_j = E_{rv}^{(j)}/\hbar\Omega$, and $E_{rv}^{(j)}$ denotes Huang–Rhys fac-

tors and the energy of the reorganization of the intramolecular high-frequency mode for the transition between the ground and U_{ej} excited state. In (9), the index $j = 1, 2$ indicates the V_{el} value in complexes obtained by the excitation of the CT1 and CT2 bands, respectively.

Let us formulate the initial conditions. Suppose that the pumping pulse is fairly narrow, and its electric field has the form $E(t) = E_0\exp(-i\Omega_e t - t^2/\tau_e^2)$. This assumption allows us to very accurately calculate the initial distribution at the U_{ej} excited term [25],

$$\rho_{ej}(Q, t = 0) = Z^{-1}\sum_n \frac{S_j^n e^{-S_j}}{n!} \times \exp\left(-\frac{\left(\Delta G_e^{(j)} + \sum_i^m (2E_{ri}^{(j)})^{1/2} Q_i\right)^2 \tau_e^2}{2\hbar^2} - \sum_i^m \frac{Q_i^2}{2k_B T} \right). \quad (10)$$

Here, $\Delta G_e^{(j)} = \hbar\Omega_e + \Delta G_{CR}^{(j)} - E_r^{(j)}$.

System (5), (6) of differential equations and initial conditions (10) determine the mathematical model of charge recombination in photoexcited donor–acceptor complexes. For comparison with the experimental data, we introduce the population of the ionic state $P(t)$ calculated as

$$P(t) = \int \rho_{e1}(Q_1, \ldots, Q_m, t) dQ_1 \ldots dQ_m. \quad (11)$$

The suggested model was tested numerically using Brownian modeling methods developed in [25, 26]; 10^5 random trajectories were used in calculations.

THE DETERMINATION OF ELECTRONIC TRANSITION PARAMETERS FROM ABSORPTION SPECTRA

The electronic term energy parameters were determined from information contained in the stationary optical absorption spectra of the TMB/TCNE complex dissolved in ACN. To separate bands and determine the contribution of each of them, the spectrum was approximated by the sum of two asymmetric Gauss functions. After this, each absorption band was approximated by the equation [27–31]

$$A_j(\omega_e) = C_j\sum_n \frac{S_j^n e^{-S_1}}{n!} \times \exp\left\{ -\frac{[\Delta G_{CR}^{(j)} - E_r^{(j)} - n\hbar\Omega - \hbar\omega_e]^2}{4E_r^{(j)} k_B T} \right\}. \quad (12)$$

At the first stage, we determined the transition energy parameters for the CT1 band, including the energy of medium reorganization $E_r^{(1)}$, the Gibbs energy of charge recombination $\Delta G_{CR}^{(1)}$, and the dimensionless Huang–Rhys parameter S_1 proportional to the reorganization energy of the intramolecular vibrational mode. The effective frequency of the intramolecular vibrational mode Ω was set at 0.17 eV, because this value was most frequently used to describe electronic transitions in aromatic donor–acceptor complexes. The best fit for CT1 was obtained at the following parameter values: $E_r^{(1)} = 1.02$ eV, $\Delta G_{CR}^{(1)} = -0.39$ eV, and $S_1 = 3.34$.

At the next stage, we determined the energy parameters related to the CT2 band. For this purpose, the optical stationary absorption spectrum was approximated by two terms of form (12). All the parameters for the CT1 band except the C_1 amplitude coefficient were determined at the preceding stage. The effective intramolecular vibration frequency for the second transition was also set at 0.17 eV. Since the CT1 and CT2 charge transfer bands characterize the same donor-acceptor complex, we must not expect the medium reorganization energies for these transitions to be strongly different. It was assumed in our calculations that the medium reorganization energies for the CT1 and CT2 transitions coincided, $E_r^{(2)} = E_r^{(1)}$. The closest agreement with the experimental spectrum was obtained with the following CT2 band parameters: $\Delta G_{CR}^{(2)} = -1.48$ eV and $S^{(2)} = 3.22$.

The experimental and calculated absorption spectra are shown in Fig. 2. Note that fairly good agreement between the theoretical and experimental data was obtained almost over the whole region of charge transfer bands. Below, these parameters are used to model the dynamics of charge recombination in excited donor–acceptor complexes.

THE DYNAMICS OF CHARGE RECOMBINATION IN EXCITED DONOR–ACCEPTOR COMPLEXES

The dynamics of charge recombination was modeled using the stochastic approach by the method of random trajectories. The energy parameters of the CT1 and CT2 electronic transitions were determined above, and the other model parameters were as follows: vibrational high-frequency mode relaxation time $\tau_v^{(1)} = 150$ fs and pumping pulse width $\tau_e = 100$ fs [17]; the dynamic characteristics of the solvents under consideration are listed in the table.

We see from Fig. 2 that a 620 nm pumping pulse only excites the CT1 band. This allows us to divide the determination of the electronic interaction parameters of two transitions, CT1 and CT2, into two stages. At the first stage, we use a two-level model to estimate the parameter for the transition from the first excited state

$|e1\rangle$ into the ground state $|g\rangle$. The V_{el1} value is selected to reproduce the dynamics of charge recombination in TMB/TCNE (ACN) after excitation by a 620 nm pulse. According to Fig. 3, the $V_{el1} = 0.08$ eV value gives close agreement between the theoretical and experimental dependences. Here, electronic interaction is fairly strong, hot transitions are very effective, and an only insignificant (almost unobservable) fraction of complexes are thermalized.

Excitation at 480 nm results in substantial overlapping of the CT1 and CT2 bands (see Fig. 2); therefore, both excited states are populated. The probability of population of one or another state at the pumping pulse wavelength λ_e can be estimated as the ratio between the absorption coefficient for the transition to this state and the total absorption,

$$W_j(\lambda_e) = A_j(\lambda_e)/A(\lambda_e), \quad (13)$$

where $A(\lambda_e) = A_1(\lambda_e) + A_2(\lambda_e)$ is the sum of the absorption coefficients at the wavelength λ_e. We assumed that the pumping pulse with a 480 nm wavelength formed wave packets on the terms U_{e1} and U_{e2} with the statistical weights W_1 (480) and W_2 (480), respectively. The initial form of both packets was calculated by (10).

The dynamics of recombination of complexes excited into the U_{e1} state was calculated as for excitation by 620 nm pulses with the same parameters. The only difference was the initial positions of the wave packets. A rapid radiationless transfer of initial distribution to the U_{e1} term occurs in complexes excited into the U_{e2} state. Recombination is then treated as the transition between the $|e1\rangle$ and $|g\rangle$ states with the parameters found for this transition above except the electronic transition matrix element. This reflects the difference between the geometries of the complexes active in the CT1 and CT2 transitions. The V_{el2} value was selected to bring the calculated dynamics of the population of the ionic state in coincidence with the experimental dynamics. The best agreement was obtained at $V_{el2} = 0.05$ eV.

We see from Fig. 3 that the model quantitatively reproduces the experimental data over the time interval presented in the figure. Note that, at times longer than 0.5 ps, a plateau appears, which, in terms of the suggested approach, is treated as the thermal stage. The height of the plateau is determined by the relative number of complexes that avoided hot recombination. The thermal stage of the decay of the excited state has a much lower effective rate. The characteristic reaction time at this stage was found to be $\tau_{eff} = 50$ ps. It was, however, shown experimentally that the population of the ionic state at times from 0.5 to 100 ps remained almost unchanged [17]; that is, the characteristic reaction time was much longer than 50 ps. This difference could be caused by the solvation of ions ignored in our theory. Solvation that occurs in the picosecond region increases the interionic distance, which decreases V_{el2} and decelerates recombination.

Relaxation times τ_i and the corresponding weights x_i for the solvents under consideration

Solvent	τ_1	τ_2	x_1	x_2
Acetonitrile	0.19	0.5 [27]	0.5	0.5
Valeronitrile	0.19	4.7 [32]	0.5	0.5
Octanonitrile	0.19	6.4 [32]	0.23	0.77

The dynamics of recombination of complexes excited by 530 nm pulses is shown in Fig. 3. These calculation results also closely agree with the experimental data (not shown in the figure).

Note that our study revealed a weak dependence of the results on the energy of medium reorganization for transitions into the second excited state $E_r^{(2)}$. Quite satisfactory agreement of both the stationary absorption spectrum and the dynamics of recombination with the experimental data was obtained when this value was varied over a fairly broad range, 0.3 eV < $E_r^{(2)}$ < 1.0 eV. Over this range, the electronic interaction parameters V_{el1} and V_{el2} changed insignificantly. This means that the true $E_r^{(2)}$ value can be noticeably different from that selected in this work.

Calculations of the charge recombination dynamics in TMB/TCNE in slower solvents, valeronitrile and octanonitrile, showed that the effectiveness of the hot stage increased and the thermal stage became unobservable, which was in complete agreement with the experimental data [17]. This was an expected behavior,

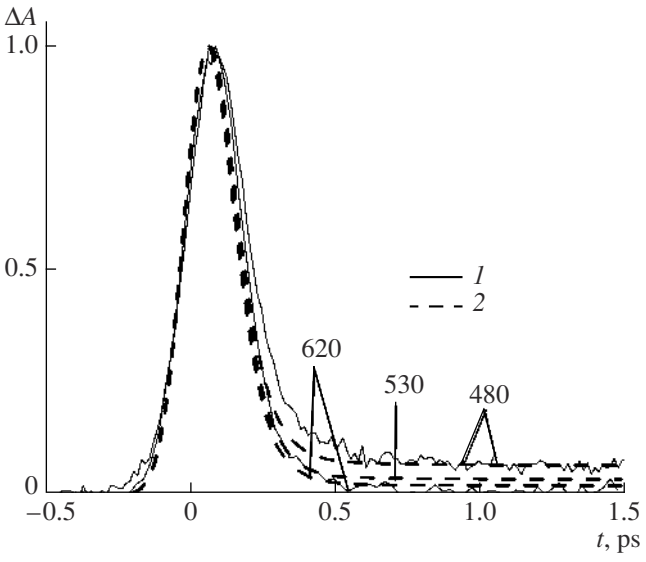

Fig. 3. Time dependence of the population of the excited state of the TMB/TCNE complex in ACN: (*1*) experimental and (*2*) obtained in numerical modeling. Numbers are pumping pulse wavelengths.

because the probability of nonthermal transitions at each intersection between the $U_g^{(n)}$ and U_{e1} terms increased as the relaxation time of the solvent grew longer [33].

We used fairly large electronic transition matrix element V_{elj} values. This requires an inquiry into the conditions of theory applicability, because the stochastic approach is only valid at fairly low V_{elj} values. It should, however, be borne in mind that the high-frequency vibrational mode decreases the effective electronic matrix element value at the expense of the Frank–Condon factor. It was shown in [11–13] that the overwhelming majority of hot transitions occurred into vibrational states with large quantum number n values, for which the condition of theory applicability $V_{nj} < k_B T$ was fulfilled.

To summarize, we showed that the two-step dynamics of charge recombination observed experimentally for complexes consisting of TMB and TCNE [17] reflected the presence of two recombination stages, hot and thermal. This experimental observation was direct evidence in favor of the nonthermal mechanism of charge recombination in excited donor–acceptor complexes described by model A.

It is likely that the reason for the observation of two-step recombination dynamics only for complexes with two charge-transfer absorption bands is as follows. Donor–acceptor complexes are fairly labile systems and can exist in several quasi-equilibrium configurations. Complexes with one charge-transfer band largely absorb radiation in configurations with the largest electronic matrix element of transition to the ionic state. This is obvious, because the probability of absorption is proportional to the square of this matrix element. A large matrix element value results in superfast charge recombination, which ends already at the hot stage. Complexes with two absorption bands have different optimum geometries corresponding to maximum electronic matrix element values for transitions into the first and second excited state. As a result, the geometry of a donor–acceptor complex that underwent the transition to the second excited state and radiationless transition to the first excited state is not optimum for subsequent charge recombination. A smaller transition matrix element value results in incomplete charge recombination at the nonthermal stage and, as a consequence, the second thermal recombination stage becomes observable.

ACKNOWLEDGMENTS

The authors thank S.V. Fes'kov for providing the program for calculations. This work was financially supported by the Russian Foundation for Basic Research, project no. 08-03-00534.

REFERENCES

1. A. M. Kuznetsov, *Charge Transfer in Physics, Chemistry, and Biology* (Gordon & Breach, Amsterdam, 1995).
2. T. Asahi and N. Mataga, J. Phys. Chem. **93**, 6575 (1989).
3. T. Asahi and N. Mataga, J. Phys. Chem. **95**, 1956 (1991).
4. H. Segawa, C. Takehara, K. Honda, et al., J. Phys. Chem. **99**, 503 (1992).
5. C. A. Benniston, A. Harriman, D. Philp, and J. F. Stoddart, J. Am. Chem. Soc. **115**, 5298 (1993).
6. I. R. Gould, D. Noukakis, L. Gomez-Jahn, et al., J. Am. Chem. Soc. **115**, 4405 (1993).
7. S. M. Hubig, T. M. Bockman, and J. K. Kochi, J. Am. Chem. Soc. **118**, 3842 (1996).
8. O. Nicolet and E. Vauthey, J. Phys. Chem. A **106**, 5553 (2002).
9. R. A. Marcus, J. Phys. Chem. A **24**, 966 (1956).
10. M. Tachiya and S. Murata, J. Am. Chem. Soc. **116**, 2434 (1994).
11. S. V. Feskov, V. N. Ionkin, and A. I. Ivanov, J. Phys. Chem. A **110**, 11919 (2006).
12. A. I. Ivanov, V. N. Ionkin, and S. V. Fes'kov, Zh. Fiz. Khim. **82** (2), 374 (2008) [Russ. J. Phys. Chem. A **82** (2), 303 (2008)].
13. S. V. Feskov, V. N. Ionkin, A. I. Ivanov, et al., J. Phys. Chem. A **112**, 594 (2008).
14. P. A. Frantsuzov and M. Tachiya, J. Chem. Phys. **112**, 4216 (2000).
15. V. A. Mikhailova, A. I. Ivanov, and E. Vauthey, J. Chem. Phys. **121**, 6463 (2004).
16. A. I. Ivanov and V. A. Mikhailova, Zh. Fiz. Khim. **80** (6), 1053 (2006) [Russ. J. Phys. Chem. **80** (6), 922 (2006)].
17. O. Nicolet, N. Banerji, S. Pages, and E. Vauthey, J. Phys. Chem. A **109**, 8236 (2005).
18. E. M. Voigt, J. Am. Chem. Soc. **86**, 3611 (1964).
19. S. Garg and C. Smyth, J. Phys. Chem. **69**, 1294 (1965).
20. R. Jimenez, G. R. Fleming, P. V. Kumar, and M. Maroncelli, Nature (London) **369**, 471 (1994).
21. P. J. Reid and P. F. Barbara, J. Phys. Chem. **99**, 17311 (1995).
22. H. Risken, *The Fokker-Planck Equation* (Springer, Berlin, 1989).
23. L. D. Zusman, J. Chem. Phys. **49**, 295 (1980).
24. A. I. Burshtein and B. I. Yakobson, J. Chem. Phys. **49**, 385 (1980).
25. R. G. Fedunov, S. V. Feskov, A. I. Ivanov, et al., J. Chem. Phys. **121**, 3643 (2004).
26. V. Gladkikh, A. I. Burshtein, S. V. Feskov, et al., J. Chem. Phys. **123**, 244510 (2005).
27. G. C. Walker, E. Akesson, A. E. Johnson, et al., J. Phys. Chem. **96**, 3728 (1992).
28. I. R. Gould, D. Noukakis, L. Gomez-Jahn, et al., J. Am. Chem. Soc. **115**, 3830 (1993).
29. I. R. Gould, D. Noukakis, J. L. Goodman, et al., Chem. Phys. **176**, 439 (1993).
30. K. Wynne, C. Galli, and R. M. Hochstrasser, J. Chem. Phys. **100**, 4797 (1994).
31. K. Wynne, G. D. Reid, and R. M. Hochstrasser, J. Chem. Phys. **105**, 2287 (1996).
32. J. C. Gumy, O. Nicolet, and E. Vauthey, J. Phys. Chem. A **103**, 10737 (1999).
33. A. I. Ivanov and V. V. Potovoi, Chem. Phys. **247**, 245 (1999).